

MIT Open Access Articles

Seeded growth of boron arsenide single crystals with high thermal conductivity

The MIT Faculty has made this article openly available. **Please share** how this access benefits you. Your story matters.

Citation: Tian, Fei et al. "Seeded Growth of Boron Arsenide Single Crystals with High Thermal Conductivity." Applied Physics Letters 112, 3 (January 2018): 031903 © 2018 Author(s)

As Published: <http://dx.doi.org/10.1063/1.5004200>

Publisher: AIP Publishing

Persistent URL: <http://hdl.handle.net/1721.1/120513>

Version: Final published version: final published article, as it appeared in a journal, conference proceedings, or other formally published context

Terms of Use: Article is made available in accordance with the publisher's policy and may be subject to US copyright law. Please refer to the publisher's site for terms of use.



Seeded growth of boron arsenide single crystals with high thermal conductivity

Fei Tian,¹ Bai Song,² Bing Lv,³ Jingying Sun,¹ Shuyuan Huan,¹ Qi Wu,¹ Jun Mao,^{1,4} Yizhou Ni,¹ Zhiwei Ding,² Samuel Huberman,² Te-Huan Liu,² Gang Chen,² Shuo Chen,¹ Ching-Wu Chu,¹ and Zhifeng Ren^{1,a)}

¹Department of Physics and the Texas Center for Superconductivity, University of Houston, Houston, Texas 77204, USA

²Department of Mechanical Engineering, Massachusetts Institute of Technology, Cambridge, Massachusetts 02139, USA

³Department of Physics, University of Texas at Dallas, Dallas, Texas 75080, USA

⁴Department of Mechanical Engineering, University of Houston, Houston, Texas 77204, USA

(Received 12 September 2017; accepted 29 December 2017; published online 16 January 2018)

Materials with high thermal conductivities are crucial to effectively cooling high-power-density electronic and optoelectronic devices. Recently, zinc-blende boron arsenide (BAs) has been predicted to have a very high thermal conductivity of over $2000 \text{ W m}^{-1} \text{ K}^{-1}$ at room temperature by first-principles calculations, rendering it a close competitor for diamond which holds the highest thermal conductivity among bulk materials. Experimental demonstration, however, has proved extremely challenging, especially in the preparation of large high quality single crystals. Although BAs crystals have been previously grown by chemical vapor transport (CVT), the growth process relies on spontaneous nucleation and results in small crystals with multiple grains and various defects. Here, we report a controllable CVT synthesis of large single BAs crystals ($400\text{--}600 \mu\text{m}$) by using carefully selected tiny BAs single crystals as seeds. We have obtained BAs single crystals with a thermal conductivity of $351 \pm 21 \text{ W m}^{-1} \text{ K}^{-1}$ at room temperature, which is almost twice as conductive as previously reported BAs crystals. Further improvement along this direction is very likely. *Published by AIP Publishing.* <https://doi.org/10.1063/1.5004200>

Overheating presents a major challenge in the modern electronics industry, which is characterized by ever-shrinking dimensions and increasing power density.¹ High temperatures not only limit device performance but also greatly reduce reliability and lifetime. To effectively dissipate heat from an electronic chip into the ambient, packaging materials with sufficiently high thermal conductivities are indispensable. The quest for materials with ever-higher thermal conductivities has recently been boosted by surprising theoretical prediction of Lindsay *et al.* that zinc-blende boron arsenide (BAs) may be among the most thermally conductive materials.^{2–5} Specifically, first-principles computations on BAs single crystals predicted that at room temperature, natural BAs has a thermal conductivity of over $2000 \text{ W m}^{-1} \text{ K}^{-1}$, and the value goes beyond $3000 \text{ W m}^{-1} \text{ K}^{-1}$ for isotopically pure BAs. This makes BAs comparable to diamond (about $2000 \text{ W m}^{-1} \text{ K}^{-1}$)⁶ and nearly an order-of-magnitude more conductive than some of the best traditional heat conductors such as copper ($\sim 400 \text{ W m}^{-1} \text{ K}^{-1}$)⁷ and aluminum nitride ($\sim 300 \text{ W m}^{-1} \text{ K}^{-1}$).⁸

Experimentally, however, only limited success has been reported, due to a range of challenges in the crystal growth of BAs.^{9–12} It is well known that boron compounds are hard to make in dense bulk form. Growth of single crystals is especially difficult, yet is necessary for eliminating phonon scattering caused by grain boundaries and ultimately obtaining the predicted high thermal conductivity of BAs. Besides, arsenide synthesis is challenging because of the high toxicity and

volatility of As. In addition, zinc-blende BAs decomposes into subarsenide B_{12}As_2 at around 920°C , which is far below the melting point of B ($\sim 2027^\circ\text{C}$).¹³ This substantially limits the growth of BAs crystals using conventional crystal growth routes such as flux recrystallization and zone melting.⁹ Even though the synthesis of pure zinc-blende BAs single crystals has long been sought after, it remains a great challenge to obtain BAs single crystals of macroscopic dimensions and experimentally demonstrate the predicted ultrahigh thermal conductivity. BAs crystals with dimensions up to $\sim 200 \mu\text{m}$ have been recently grown, and the thermal conductivity is measured to be only $\sim 200 \text{ W m}^{-1} \text{ K}^{-1}$ at room temperature.⁹ Further, rod-shaped BAs crystals with a diameter of around $1.15 \mu\text{m}$ have also been fabricated and characterized with a thermal conductivity of $\sim 186 \text{ W m}^{-1} \text{ K}^{-1}$.¹¹ Compared to the theoretically predicted values, the measured thermal conductivities of BAs crystals are lower by about an order of magnitude, possibly due to As deficiency, anti-site defects, voids, impurities, twin boundaries, grain boundaries, and so on.

During chemical vapor transport (CVT) growth of BAs, gaseous B-related species are first transferred from the hot end of a quartz tube to the cold end and subsequently form BAs crystals by reacting with As_4 vapor at the cold end. The supersaturation of the crystal component vapors drives the crystal growth and is controlled by the temperature difference between the source material and the crystallization front. It is worthwhile to note that defects can be easily introduced into the crystals during the growth process due to competitions between various near-energy-equivalent

^{a)}Author to whom correspondence should be addressed: zren@uh.edu

crystallization pathways.¹⁴ In order to grow crystals of large size and high quality, it is critical to properly manage the nucleation process and growth rate in the CVT process. Unfortunately, the spontaneous nucleation caused by supersaturation is normally uncontrollable. Tiny defects inside the quartz tube usually act as heterogeneous nucleation centers that initiate crystal growth. Due to the existence of these randomly distributed nucleation centers, the grown crystals are often found clustered, twisted, and tilted against each other. The structural quality of one crystal suffers from surrounding crystals since they limit space and induce stress. As a result, irregular morphology and micro-cracks are often present in typical CVT-grown BAs crystals. A possible solution to these issues is to use small BAs single crystals as seeds to better control the nucleation process and facilitate the growth of BAs single crystals with a larger size and higher quality. Note that unless the seeding is done properly (e.g., selection of seed crystals, seed distribution, and the shape and surface of the quartz tube), effective elimination of crystal defects may not be realized.¹⁵

Here, we report the synthesis of larger-size and higher quality BAs single crystals via placing tiny BAs single crystal seeds in an improved CVT system using pure B as the source material instead of traditional polycrystalline BAs precursors.^{9,10,12} First, pure As (Alfa Aesar, 99.999%) and isotopically enriched B (Alfa Aesar, 99.9%, >96%¹¹ B) with an As:B molar ratio of 1.2:1 together with some iodine (I₂, Alfa Aesar, 99.999%, ~50 mg per cm³ tube volume) were sealed in a fused quartz tube under vacuum. Subsequently, the quartz tube was placed in a horizontal two-zone tube furnace. The mixture of the source materials was placed at the high temperature zone which was held at ~890 °C to avoid decomposition of BAs. Over the course of approximately two weeks, many aggregated BAs crystals with typical sizes of 200–400 μm were found in the low temperature zone which was held at ~800 °C. These crystals were crushed into pieces. Several small (<20 μm), regularly shaped, and (111)-oriented single crystals were then carefully selected and placed at the crystal growth end of another quartz tube as seed crystals, as illustrated in Fig. 1. By repeating the growth process, we obtained some larger single crystals with much better morphology and cleaner surface thanks to seeded nucleation as compared to spontaneous nucleation. We found that excess As also forms As crystals at the cold end. Consequently, after the growth process, the crystals were

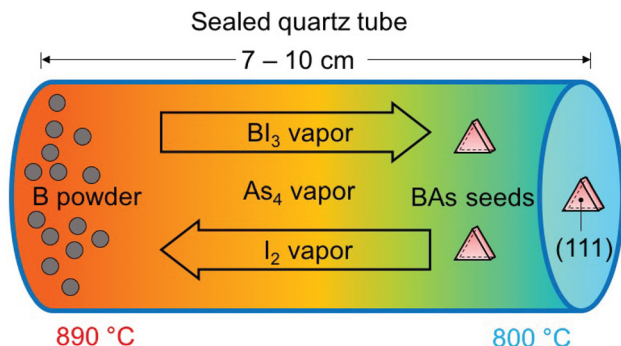
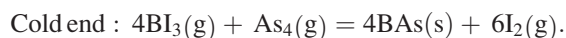
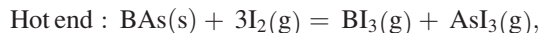


FIG. 1. Schematic diagram of BAs single crystal growth via a horizontal seeded CVT method.

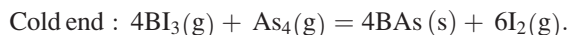
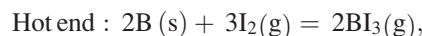
collected and etched sequentially with concentrated nitric acid (70.0%) and *aqua regia* to remove all deposits on the surface of the BAs crystals. Finally, the crystals were cleaned with ethanol and de-ionized water for further characterizations.

The crystals grown without seeds were normally 200–400 μm in size and of relatively poor quality with cracks, irregular facets, and multiple domains as shown in Fig. 2(a). By contrast, crystals grown from the seeds were bigger with a typical size of 400–600 μm, much better morphology, and cleaner surface [Figs. 2(b) and 2(c)]. Spontaneously grown crystals with a much smaller size (20–200 μm) were also found inside the quartz tube where no seeds were placed. X-ray diffraction analysis (Rigaku D-max IIIB X-Ray Diffractometer with a Cu Kα radiation source) was performed on the crystals for structural characterization (Fig. 3). The shiny flat surface with light grey metallic luster of the as-grown crystals was found to be the (111) facet, the same as the seed crystals, thus confirming the effectiveness of the seeding technique for controlling nucleation and the direction of crystal growth. The rocking curve measurement of the (111) plane showed a full width at half maximum (FWHM) of ~0.056°, indicating relatively low crystal imperfection and high quality of as-grown crystals.

In addition to proper seeding, optimization of the source material and understanding of the detailed chemical reactions are also key to the growth of high quality BAs crystals. Chu *et al.* claimed that using BAs powder as the source material would lead to faster CVT crystal growth than using pure B as the source.¹⁰ More recently, Lv *et al.* also reported that a well-prepared polycrystalline BAs precursor was a proper source material.⁹ Both of them tend to suggest that the mechanism underlying the CVT process is



In our effort to improve the crystal quality, we have systematically experimented with pure B, polycrystalline BAs powder with high As deficiency, and near-perfect (low As deficiency) polycrystalline BAs powder as the source material for CVT BAs crystal growth. We were able to collect BAs crystals at the growth end with either pure B or high As deficiency BAs precursor as the source material, but no BAs crystals were found when the BAs precursor with low As deficiency was used. Although no experimental data for the Gibbs free energy of BAs are currently available, one may draw the conclusion that at around 900 °C, I₂ can hardly react with near-perfect BAs. In light of this observation, we propose below a more probable chemical mechanism underlying the CVT growth of BAs



The thermal conductivity of our sub-millimeter sized BAs crystals was measured using a noncontact optical pump-probe technique called time-domain thermoreflectance (TDTR).^{16,17} Briefly, one heats up an aluminum-coated BAs crystal using a high-power ultrashort (100 fs) pulsed pump

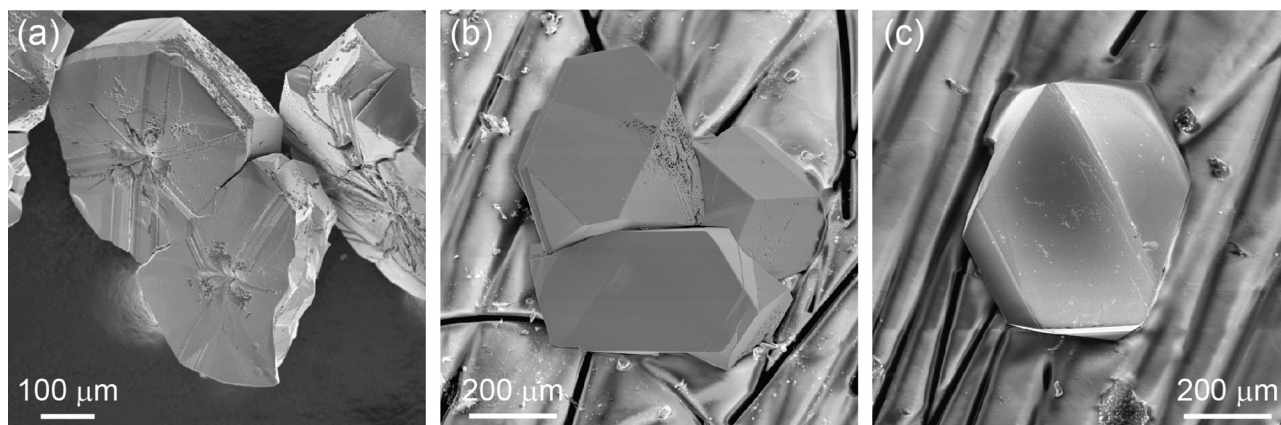


FIG. 2. SEM images of BAs crystals after cleaning with nitric acid and *aqua regia*. (a) BAs crystals with poor quality and central radiative cracks, irregular facets, and multi domains by regular self-nucleation growth. (b) and (c) As-grown BAs crystals with clean and flat surfaces by using tiny BAs single crystals as seeds.

laser and monitors the subsequent cooling process with a low-power probe pulse (100 fs, Fig. 4). The aluminum coating serves as both a laser absorber and a reflectance-based thermometer. The measured cooling curve is fitted to a Fourier heat conduction model to get the sample thermal conductivity. The pump power is usually modulated to increase the signal-to-noise ratio. This generates a complex thermoreflectance signal which is recorded using a lock-in amplifier. On the crystal shown in Fig. 2(c), thermal conductivities in the range of about $80 \text{ W m}^{-1} \text{ K}^{-1}$ to over $300 \text{ W m}^{-1} \text{ K}^{-1}$ were measured at different locations (see [supplementary material](#), Table S1). Meanwhile, we observed variations in the surface conditions and Raman spectra across the sample, which might have contributed to large variations in the measured thermal conductivity. As an example, Figs. 4(a) and 4(b) present the measured and fitted thermoreflectance curves (the ratio between the real and the imaginary part, or equivalently, the phase of the complex signal) at a select spot, which yields a thermal conductivity

as high as $351 \pm 21 \text{ W m}^{-1} \text{ K}^{-1}$ (Table S2, [supplementary material](#)). In comparison, we note that the highest thermal conductivities of the crystals shown in Figs. 2(a) and 2(b) were measured to be $55.9 \pm 0.3 \text{ W m}^{-1} \text{ K}^{-1}$ [see Fig. 4(c)] and $131 \pm 13 \text{ W m}^{-1} \text{ K}^{-1}$, respectively. The interface thermal conductance between the aluminum coating and the BAs crystal [Fig. 2(c)] was simultaneously fitted to be $81 \pm 8 \text{ MW m}^{-2} \text{ K}^{-1}$, indicating good interface quality. Changing the fitted thermal conductivity by 20% resulted in a large discrepancy between the computed and measured data, suggesting good experimental sensitivity. The fitted material properties lead to excellent agreement between computed and measured thermoreflectance signals in both the phase and the amplitude (see [supplementary material](#), Fig. S1), further confirming the experimental reliability. Additionally, the electrical conductivity was measured to be about 164 S/m using the four-probe method, and the electron thermal conductivity as estimated by the Wiedemann-Franz relationship was on the order of $1 \text{ mW m}^{-1} \text{ K}^{-1}$. Although the measured thermal conductivity is an order-of-magnitude lower than the theoretical predictions for single crystal BAs, this value is higher than any of the previously reported values for single crystal BAs and comparable to the highest thermal conductivities from traditional heat conductors.

The large discrepancy between the measured and predicted thermal conductivities, combined with the relatively large variation of thermal conductivity across the same crystal, suggests that despite the improved growth technique and crystal quality, some defects may still exist, such as As deficiency, impurities, voids, and grain boundaries. For example, it was recently predicted that for BAs crystals to have a room temperature thermal conductivity over $1000 \text{ W m}^{-1} \text{ K}^{-1}$, an As vacancy of less than $3 \times 10^{18} \text{ cm}^{-3}$ is required.¹⁸ However, it remains a non-trivial experimental challenge to identify and quantify these possible defects, particularly due to difficulties in detecting B atoms. Temperature-dependent thermal conductivity measurements are currently being pursued to help identify the scattering mechanisms. Considering the fact that some small crystals with poor quality were still found at locations without seeds during the seeded growth, there is clearly room to improve the seeded CVT growth technique. As a result, we are in the process of further suppressing

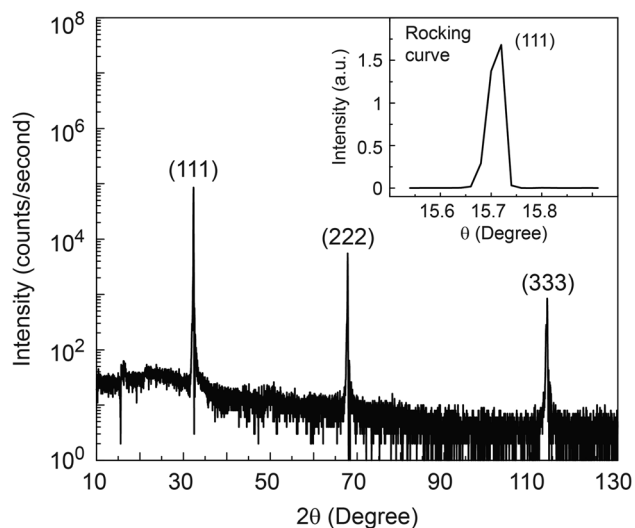


FIG. 3. X-ray diffraction pattern taken from a shiny and flat surface with light grey metallic luster on a selected BAs single crystal by the seeded CVT method shows the preferred orientation of (111). The rocking curve of the (111) peak (inset) shows the full width at half maximum (FWHM) of 0.056° . The refined lattice parameter is $a = 4.7859(5) \text{ \AA}$.

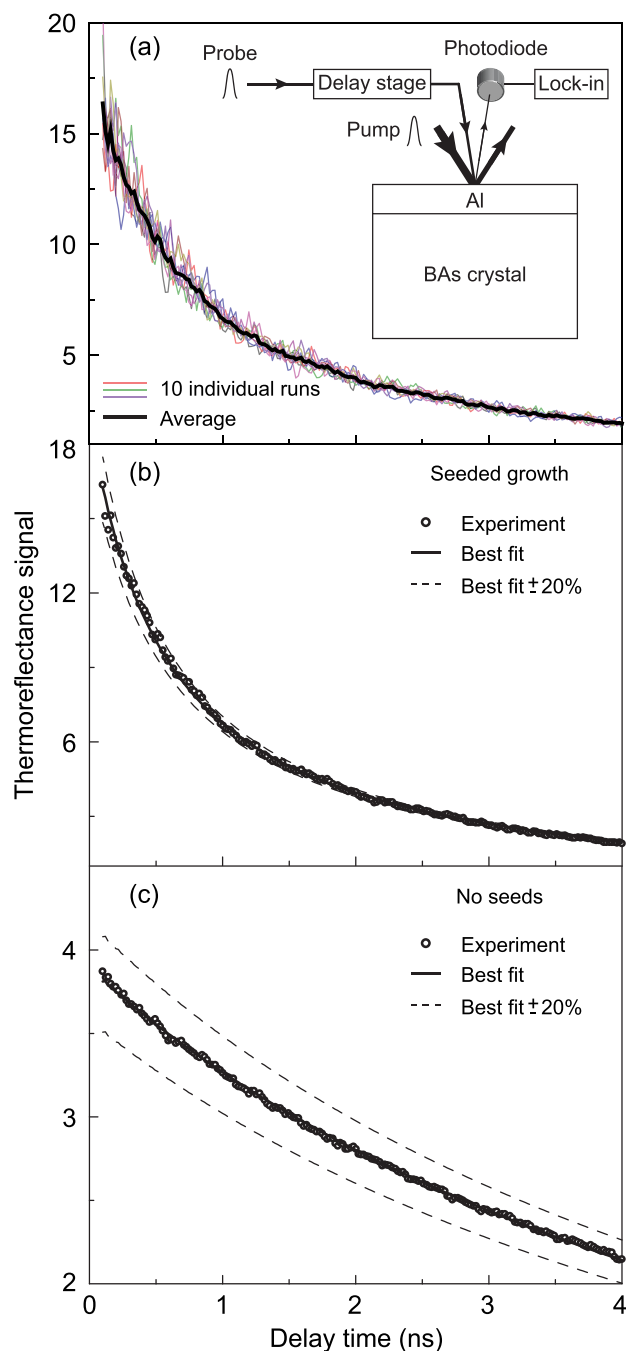


FIG. 4. Thermal conductivities of BA crystals measured using TDTR. (a) Ten representative thermorefectance curves and their average from the crystal shown in Fig. 2(c). (b) shows the results of directly fitting (solid line) the average experimental data (circles), which yields a thermal conductivity of $341 \text{ W m}^{-1} \text{ K}^{-1}$. The dashed lines indicate how much the computed thermorefectance signal deviates from experimental data if the thermal conductivity was changed by 20% from the best fit values. (c) Only $56 \text{ W m}^{-1} \text{ K}^{-1}$ was measured from the crystal in Fig. 2(a).

spontaneous nucleation on the tube walls. In addition, efforts are being made to understand more thoroughly the thermodynamics of the growth process in order to better control it and to ultimately grow BA single crystals of macroscopic size with significantly improved thermal conductivity. On the other hand, computations incorporating increasingly more detailed microscopic scattering processes (e.g., four-phonon scattering and electron-phonon scattering) are being pursued, which usually lead to lower

calculated thermal conductivities and would potentially explain part of the discrepancy.

To summarize, compared with previous reports, BA single crystals with a larger size ($400\text{--}600 \mu\text{m}$), better morphology, and higher quality were obtained by placing tiny BA single crystals as seeds in an improved CVT system in this work. These higher quality single crystals indeed demonstrate a higher thermal conductivity of about $351 \text{ W m}^{-1} \text{ K}^{-1}$ at room temperature, which is about twice as high as previously reported experimental values for BA crystals. The seeds played a key role in the growth process, especially for the crystal size and quality. Further improvement is very promising.

See [supplementary material](#) for more details on the thermal conductivity measurements.

This work was funded by the Office of Naval Research under a MURI Grant N00014-16-1-2436, U.S. Air Force Office of Scientific Research Grant FA9550-15-1-0236, the T. L. L. Temple Foundation, the John J. and Rebecca Moores Endowment, and the State of Texas through the Texas Center for Superconductivity at the University of Houston.

¹A. L. Moore and L. Shi, “Emerging challenges and materials for thermal management of electronics,” *Mater. Today* **17**(4), 163–174 (2014).

²L. Lindsay, D. A. Broido, and T. L. Reinecke, “First-principles determination of ultrahigh thermal conductivity of boron arsenide: A competitor for diamond?,” *Phys. Rev. Lett.* **111**(2), 025901 (2013).

³D. A. Broido, L. Lindsay, and T. L. Reinecke, “Ab initio study of the unusual thermal transport properties of boron arsenide and related materials,” *Phys. Rev. B* **88**(21), 214303 (2013).

⁴L. Lindsay, D. A. Broido, J. Carrete, N. Mingo, and T. L. Reinecke, “Anomalous pressure dependence of thermal conductivities of large mass ratio compounds,” *Phys. Rev. B* **91**(12), 121202 (2015).

⁵H. Ma, C. Li, S. Tang, J. Yan, A. Alatas, L. Lindsay, B. C. Sales, and Z. Tian, “Boron arsenide phonon dispersion from inelastic x-ray scattering: Potential for ultrahigh thermal conductivity,” *Phys. Rev. B* **94**(22), 220303 (2016).

⁶L. Wei, P. K. Kuo, R. L. Thomas, T. R. Anthony, and W. F. Banholzer, “Thermal conductivity of isotopically modified single crystal diamond,” *Phys. Rev. Lett.* **70**(24), 3764–3767 (1993).

⁷P. I. Frank, P. D. David, and L. B. Theodore, *Fundamentals of Heat and Mass Transfer* (John Wiley and Sons, New York, 1996).

⁸G. A. Slack, “Nonmetallic crystals with high thermal conductivity,” *J. Phys. Chem. Solids* **34**(2), 321–335 (1973).

⁹B. Lv, Y. Lan, X. Wang, Q. Zhang, Y. Hu, A. J. Jacobson, D. Broido, G. Chen, Z. Ren, and C.-W. Chu, “Experimental study of the proposed super-thermal-conductor: BAs,” *Appl. Phys. Lett.* **106**(7), 074105 (2015).

¹⁰T. L. Chu and A. E. Hyslop, “Crystal growth and properties of boron monoarsenide,” *J. Appl. Phys.* **43**(2), 276–279 (1972).

¹¹J. Kim, D. A. Evans, D. P. Sellan, O. M. Williams, E. Ou, A. H. Cowley, and L. Shi, “Thermal and thermoelectric transport measurements of an individual boron arsenide microstructure,” *Appl. Phys. Lett.* **108**(20), 201905 (2016).

¹²H. Schäfer, *Chemical Transport Reactions* (Elsevier, 2016).

¹³J. A. Perri, S. La Placa, and B. Post, “New group III-group V compounds: BP and BAs,” *Acta Crystallogr.* **11**(4), 310 (1958).

¹⁴P. Cubillas and M. W. Anderson, “Synthesis mechanism: Crystal growth and nucleation,” in *Zeolites and Catalysis* (Wiley-VCH Verlag GmbH & Co. KGaA, 2010), pp 1–55.

¹⁵S. Kasap, *Springer Handbook of Electronic and Photonic Materials* (Springer Science & Business Media, 2006).

¹⁶D. G. Cahill, “Analysis of heat flow in layered structures for time-domain thermorefectance,” *Rev. Sci. Instrum.* **75**(12), 5119–5122 (2004).

¹⁷A. J. Schmidt, X. Chen, and G. Chen, “Pulse accumulation, radial heat conduction, and anisotropic thermal conductivity in pump-probe transient thermorefectance,” *Rev. Sci. Instrum.* **79**(11), 114902 (2008).

¹⁸N. H. Protik, J. Carrete, N. A. Katcho, N. Mingo, and D. Broido, “Ab initio study of the effect of vacancies on the thermal conductivity of boron arsenide,” *Phys. Rev. B* **94**(4), 045207 (2016).